RSC Advances

PAPER

View Article Online
View Journal | View Issue

Cite this: *RSC Adv.*, 2024, **14**, 11706

Biomass screening for syngas production by flash photopyrolysis†

Abderrahman Mellalou, [a] Wanderson O. Silva, [b] Mathieu Soutrenon, [b] Hubert H. Girault, [c] Abdelkader Outzourhit, [d] Jones Alami [a] and Fouad Ghamouss *[a]

Received 10th March 2024
Accepted 6th April 2024

DOI: 10.1039/d4ra01845a

rsc.li/rsc-advances

A few seconds flash photopyrolysis is used as efficient screening tool for the investigation of selected biomass in producing syngas, hydrogen and biochar. This innovative approach allowed rapid pyrolysis of the biomass, which was followed by a precise gas analysis and quantification, using Mass Spectrometry (MS). The analysis of the gas composition from three distinct biomass wastes in this study provides new insights into their thermochemical characteristics, expanding thus our knowledge of the potential of the selected biomass resources for the production of carbon, syngas, and/or hydrogen-rich gas production. This enhanced characterization revealed the potential of biomass transformation in contributing to innovative green energy sustainable solutions.

Introduction

Biomass is a readily accessible and abundantly available renewable energy resource on Earth, and may play a major role in the sustainable energy production landscape.[1] Globally recognized as the fourth most abundant energy resource, biomass contributes to over 10% of the total energy supply.[2] Biomass research has recently attracted growing attention, driven by the evident potential of waste-to-energy conversion.[3]

Biomass can be primarily used to produce electricity/heat energy, transport fuels and synthetic hydrogen-rich gas commonly known as syngas,[4] composed primarily of CO and H_2. In addition to its direct use as a fuel in power generation and transportation, syngas is also a potential feedstock for chemical production.[5] Notably, about 50% of the total syngas produced is directed towards ammonia production, with an additional 25% dedicated to hydrogen production.[6] The remaining portion is used in the production of methanol and hydrocarbons, exemplified by processes such as Fischer–Tropsch synthesis.[7]

Hydrogen is recognized as one of the most versatile energy carriers, as it is demonstrated to meet a wide range of energy needs across various sectors.[8] Its inherent potential for emission-free utilization is promising in the reduction of air pollutants and greenhouse gas emissions, thereby contributing to the attenuation of the environmental effects associated with traditional fossil fuels. Indeed, the viability of hydrogen as a pivotal element in the transition to a cleaner energy has been justified through extensive research and experimentation.[5,6,8] Its application in industries spanning transportation, power generation, and industrial processes highlights its potential to revolutionize the way energy is sourced and utilized.[9] Moreover, ongoing advancements in hydrogen production, storage, and distribution technologies further solidify its position as a pivotal energy vector for the future.

Syngas or hydrogen rich-gas stands out as a versatile precursor for various industrial applications, serving as a vital raw material for synthesizing fuels, chemicals, and fertilizers. Its significance lies in its potential to mitigate carbon emissions by enabling the production of clean fuels and chemicals from renewable resources. Syngas gas can be derived from diverse primary energy sources, including coal, natural gas and biomass.[5] Primary, non-renewable and GHG emitting feedstock, namely, coal and petroleum residues together with coke are the main raw materials traditionally used in gasification and steam reforming processes for syngas production.[10] However, the urgent need for the transition towards a circular economy has boosted the search for carbon neutral, highly efficient, environmentally friendly, and sustainable alternatives. Biomass is recognized as a renewable and sustainable source for producing syngas. This can be achieved primarily through thermochemical methods such as pyrolysis and gasification, as well as biological techniques like fermentation and anaerobic digestion.[11]

There is a variety of biomass feedstocks that emanate from organic wastes such as agricultural crop residues, wood,

[a]*Materials Science Energy and Nanoengineering Department, Mohamed VI Polytechnic University, Benguerir, Morocco. E-mail: Fouad.ghamouss@um6p.ma*
[b]*Institute of Systems Engineering, HES-SO Valais-Wallis, CH-1950 Sion, Switzerland*
[c]*Institut des Sciences et Ingénierie Chimiques (ISIC), École Polytechnique Fédérale de Lausanne (EPFL), Station 6, CH-1015 Lausanne, Switzerland*
[d]*Laboratory of Materials, Energy and Environment, Faculty of Sciences Semlalia, Cadi Ayyad University, Morocco*

† Electronic supplementary information (ESI) available. See DOI: https://doi.org/10.1039/d4ra01845a

municipal waste, and wet waste such as crop residues, forest residues, algae, and various industrial byproducts, including wastewater.[12] In Morocco, the agricultural sector contributes significantly to organic waste production, generating approximately 65 million tons per year.[13] This estimate relies on residue production per hectare drawn from prior studies and research findings by the FAO.[14] However, these ratios are subject to various influencing factors, including edaphic and climatic conditions, as well as cultural practices.[13] The potential energy yield achievable through the utilization of this biomass and waste amounts to approximately 13 million MW h per year, comprising 6.6 million MW h from the agricultural sector, 3.5 million MW h from forestry activities, and 3.3 million MW h from waste resources.[14]

Among the above mentioned biomass conversion methods, thermochemical processes emerge as particularly promising pathways for converting biomass into syngas.[8,11] Specifically, pyrolysis, which involves the decomposition of biomass in the absence of oxygen, and gasification, a process that converts biomass into a gas mixture primarily composed of hydrogen, carbon monoxide, and carbon dioxide, have demonstrated significant potentials.[15]

While pyrolysis focuses on the thermal breakdown of biomass, gasification revolves around the transformation of biomass into a gaseous form. However, an essential prerequisite for demonstrating the syngas production potential and maximizing syngas yield of biomass lies in effectively categorizing and classifying diverse biomass feedstocks. In this regard, photopyrolysis emerges as a promising screening technique to reveal the capabilities of various biomass materials for syngas and hydrogen rich gas production.[16]

Photopyrolysis is a non-thermal surface process that uses high power pulsed xenon light (μs to ms) to decompose biomass, such as banana peel into syngas and porous carbon.[16] Recent work demonstrated that this technique can also be used to produce hydrogen from tires.[17] Through the application of light pulses characterized by varying intensities and a wide range of wavelengths, a succession of photo-thermal and photochemical reactions is initiated. Originally designed for photonic sintering, this pulsed light system saw its first application in drying edge-oxidized graphene nanosheet films for rapid establishment of a compact electrode surface.[18] Another application was the synthesis of molybdenum carbides (Mo_2C)-based electrocatalysts on a carbon cloth substrate under ambient conditions *via* photonic flash synthesis (PFS) from a MoO_3/graphene precursor.[19] The pulsed light treatment facilitated the effective thermal decomposition of molybdenum oxides into a porous β-Mo_2C nanostructure with impressively high catalytic stability. Xenon flashlamp units are, otherwise, widely used in diverse domains including, photonic sintering,[20] surface treatment, food processing,[21] and more.

In this context, the present research is a comprehensive investigation of photo-pyrolysis as a screening tool to evaluate syngas production potential of different biomass feedstocks. More specifically, photopyrolysis effectiveness to evaluate the capacity of various Moroccan biomass sources to yield syngas and in particular hydrogen is demonstrated.

Materials and methods

Various biomass feedstocks were used in order to evaluate the potential of photo-pyrolysis as a screening tool for syngas and hydrogen rich gas production.

Feedstocks description

Pennisetum villosum, commonly referred to as feathertop grass or simply feathertop, represents a flowering plant belonging to the *Poaceae* family, as depicted in Fig. 1a. Indigenous to northeastern Africa and certain regions of the Arabian Peninsula, this species is also cultivated as an ornamental plant in various other locations. Instances of its spontaneous growth beyond cultivation are occasionally encountered. The plant's inflorescence is characterized by a panicle housing clustered spikelets enveloped by a mist-like assembly of plumose white bristles, measuring up to 5 centimeters in length.

Pennisetum alopecuroides (Fig. 1b), a member of the grass family (*Poaceae*), traces its origins to Africa (1913). Centuries ago, it was introduced as animal fodder across South America, Asia, and Australia. In Morocco, these plants thrives abundantly, notably within urban areas along roadways, often attaining heights of up to 75 cm and 2 meters, respectively. Annually, substantial quantities of *Pennisetum villosum* and *Pennisetum alopecuroides* plants are generated as a byproduct of public green space maintenance, often discarded on the city's open surfaces or employed as fuel in traditional baths (Hammams).

Onions (*Allium cepa* L.) holds a significant position among all horticultural commodities and ranks second only to tomatoes in terms of global production.[22] Worldwide onion production amounts to approximately 64.5 million tons, covering an agricultural field area of about 3.45 million ha. According to data from the National Horticulture Research and Development Foundation, Moroccan onion production is projected to reach 962 680 metric tons by 2026, with an average annual productivity growth rate of 0.8%.[23] Furthermore, onions stand out as one of the most export-oriented vegetable categories in Morocco, ranking third among the most exported vegetables. The exportation rate usually peaks during July and August, but declines significantly after February. Consequently, post-harvest waste (Petiole and Flower), Fig. 1c, from onions can amount to a significant quantities, averaging 0.5 kg per kg of

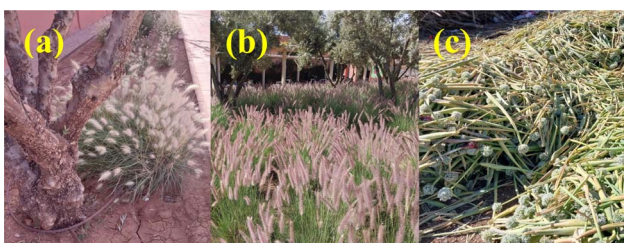

Fig. 1 Photograph of (a) *Pennisetum villosum* (b) the *Pennisetum alopecuroides* and (c) the onion post-harvesting waste (Petiole and Flower).

produced onions. In general, onion waste can be categorized into three main types: industrial waste, domestic waste, and post-harvest or supply chain waste. This waste has gained significant attention in recent years due to its potential applications in various fields, ranging from agriculture to biotechnology. However, because of its high sulfur content and strong aroma, it cannot be valorized as soil amendment. Nonetheless, it contains rich reserves of fiber, minerals, and bioactive compounds that can be recovered to develop various bioproducts, such as bioenzymes and polyphenols.[24]

Given its abundant cellulose content, these waste materials can be potentially used either as a sustainable biofuel through direct combustion or as a resource for syngas or hydrogen-rich gas production *via* thermochemical techniques like pyrolysis and gasification.

Therefore, as part of the present study, we conducted a comprehensive chemical, and physical assessment of Moroccan *Pennisetum alopecuroides*, *Pennisetum villosum* and onion waste (petiole and flower) with a specific focus on its applicability within the field of bioenergy, notably for syngas and hydrogen rich-gas generation.

All samples were collected in the Marrakech region during the spring season, subsequently ground to finer particles before drying, and characterized according to the procedures outlined below. The biomass samples were dried according to the ASTM E1756-08 standard until no weight variation was observed. However, it is important to note that during biomass storage, the moisture content may increase due to ambient humidity. Additionally, during the drying process, only the non-bound water is evaporated, leaving some water molecules within the structure of the biomass samples.

Physical and chemical characterization of feedstocks

The cellulose composition of biomass samples was assessed following the procedure outlined by Kushner and Hoffer.[25] Briefly, the samples were immersed in a solution containing nitric acid and ethanol in a 1 : 4 ratio for a duration of 4 hours. Subsequently, the samples were dryed in an oven set at 60 °C until a consistent weight was achieved. The quantification of cellulose content (%cellulose $= m_2/m_1 \times 100$) was calculated with m_1 the mass of the samples before treatment, and m_2 after treatment.

The quantification of lignin content followed the ASTM D 1106-96 standard methodology.[26] Biomass samples underwent treatment with an ethanol–toluene mixture at a ratio of 1 : 2 for a duration of 8 hours, with subsequent measurement of their mass. Subsequently, 1 gram of the biomass samples was stirred in a 15 mL solution of 72% sulfuric acid (H_2SO_4) for 2 hours. Following this, 560 mL of distilled water was introduced, and the mixture was subjected to 4 hours of boiling. The residue from this hydrolysis process was filtered *via* vacuum suction, washed with 500 mL of heated water to eliminate all acid traces, and subsequently dried in an oven maintained at 100 ± 2 °C for a period of 2 hours. The proportion of extracted lignin was determined (%lignin $= m_2/m_1 \times (100 - m_3)$), with m_1 and m_2 the masses of biomass samples before and after treatment, and m_3 the mass obtained after the solubility test of the fibers in the ethanol–toluene mixture (%).

The quantification of hemicellulose content was based on the procedure established by Boopathi *et al.*[27] Biomass samples underwent immersion in a 5% NaOH solution at room temperature for a duration of 30 minutes, followed by neutralization using an HCl solution. Ultimately, the fibers were subjected to drying in an oven set at 105 °C for 2 hours. The resulting change in weight from this process yielded the hemicellulose content, %hemicellulose $= (m_1 - m_2) \times 100$, with m_1 and m_2 the masses of the fibers before and after treatment. Each one of these experiments was repeated 5 times and the mean values were reported.

The infrared spectra of raw biomass waste were recorded using a PerkinElmer Fourier transform infrared spectrophotometer in the wavenumber range 4000–400 cm^{-1}. For this purpose, 2 mg of each biomass waste was ground into small particle and mixed with KBr.

The XRD tests were performed using a Bruker D8 discover diffractometer at 40 kV and 30 mA at room temperature. This system has a rotating anode generator with a copper target radiation source ($\lambda = 1.5406$ Å). The (2θ) angle was scanned between 5° and 80°.

The ultimate analysis was carried out using an EA3000 elemental analyzer (shimatzu Eurovector 3000). The procedure involved combustion of the measured biomass sample under a controlled atmosphere, followed by analysis of the resulting gas products, to quantify carbon, hydrogen, nitrogen, sulfur, and oxygen contents in the samples. These ultimate analyses are conventionally presented on either a dry biomass basis or a dry ash-free basis.

Thermal stability of biomass wastes was examined using a Netzsch TGA/DSC thermogravimetric analyzer. The raw feedstocks were grounded and samples of 20 mg of each feedstock were placed in a crucible and heated from 25 °C to 900 °C at a rate of 5 °C per minute under a constant flow of nitrogen, ensuring an inert atmosphere during pyrolysis.

Proximate analysis provides information on the amount of moisture, ash, volatile matter, and fixed carbon present in a biomass sample. The thermogravimetric analysis method is commonly used for proximate analysis to save analysis time. The determination of moisture, volatile matter, and ash by thermogravimetric analysis (TGA) is covered by the ASTM standard D7582-15, which involves recording the continuous weight loss of the sample as it is heated. The TGA method for proximate analysis is described in the ESI.†

The calorific values of the biomass waste samples were determined using the ultimate analysis based on the following equation[28] (HHV (MJ kg^{-1}) = 0.2949%C + 0.8250%H), where HHV represents the higher heating value, %C and %H represent the carbon and hydrogen content, respectively.

Photopyrolysis process setup and procedure

Pulsed light setup description. The experimental configuration of the pulsed light system used for biomass waste photopyrolysis is illustrated in Fig. 2. The system consists of a simple

stainless steel reactor sealed with a transparent window (borosilicate glass or quartz), which allows the biomass samples to be exposed to the high-power flash light from a Xenon lamp shown in (Fig. S1†), in an inert atmosphere (argon). The reactor is placed on a heat-resistant table (Fig. S1,† inset 1) and then exposed to the flashing irradiation (Fig. S1,† inset 2) in controlled conditions of charging voltage, exposure time, pulse shape, *etc.*, using a PulseForge 1300 photonic curing system (Novacentrix, USA).

Three biomass wastes, *i.e. Pennisetum alopecuroides*, *Pennisetum villosum* and onion waste 'petiole and flower', were selected. They were dried at 105 °C for 24 h, in order to eliminate any residual water and moisture, then ground and sieved. The resulting fine powder was subsequently utilized for further analysis.

The photo-pyrolysis utilized flash-light irradiation in the form of 5 apparent flashes of 14.5 ms each, corresponding to a total exposure of 72.5 ms. The apparent flashes were separated by 3 seconds gaps providing a total flashing time of 12.2 s and an energy input of 13.1 J cm^{-2} each pulse. This energy-intensive light pulse was applied onto the loaded biomass, reducing the biomass into biochar as illustrated in Fig. 2. A comprehensive description of this apparatus and the flashing procedure can be found in a previous work.[16]

The exhaust gases were analyzed using a PrismaPlus mass spectrometer (OMNISTAR GSD 320, Pfeifer), equipped with an yttriated iridium filament. This step aimed to qualitatively identify the gaseous products resulting from the photo-pyrolysis of the diverse natural biomass wastes. The system configuration included a metallic tube outlet containing the generated gases, which was directly connected to the mass spectrometer's gas inlet *via* a stainless-steel capillary. The mass spectrometer gas sampling line was maintained at a regulated temperature of 200 °C over a length of 1 meter.

Results and discussion

Primary characterization

The chemical composition together with the ultimate and proximate analysis of the onion waste, the *Pennisetum alopecuroides* and the *Pennisetum villosum* without preliminary drying are presented in Table 1. Proximate analysis revealed that for all three materials, significant variations of moisture content, volatile matter, ash, and fixed carbon were detected. Onion waste exhibited the lowest moisture content (44.19%), while *Pennisetum alopecuroides* displayed lower ash (4.76%) and fixed carbon (5.02%) percentages, making it a potentially an attractive material for thermochemical conversion processes, namely syngas and hydrogen rich-gas production. *Pennisetum villosum* showed a moderate moisture (54.89%) and volatile matter (31.54%) levels, offering a balanced composition for diverse biorefinery applications. The investigated biomass wastes exhibited a varying ash content due to the presence of different types of inorganic elements. *Pennisetum alopecuroides* and *Pennisetum villosum* exhibit, otherwise, high mineral contents, attributed to their elevated ash content.

Ultimate analysis yielded the elemental compositions in each of the studied samples, with *Pennisetum villosum* exhibiting elevated nitrogen (2.32%) and oxygen (53.33%) contents compared to the other two substrates. Onion waste exhibited a carbon content of 45.11%, making it a potential carbon-rich feedstock for pyrolysis-based applications. Moreover, cellulose, hemicellulose, and lignin contents were characterized to understand the biomass structure and its implications for processing. *Pennisetum alopecuroides* exhibited the highest cellulose content with a weight percentage of 42.53%, compared to *Pennisetum villosum* and onion waste with the corresponding percentages of 32.23% and 29.37%, respectively. The cellulose content of *Pennisetum alopecuroides* is close to that of Alfa,[29] which, as a consequence, makes it a promising candidate for cellulose-based materials. *Pennisetum villosum*, on the other hand, demonstrated a remarkably high hemicellulose content (51.62%), making it a promising candidate for hemicellulose-derived value-added products. Additionally, the lignin content was relatively low in *Pennisetum villosum* (12.42%), potentially reducing the challenges associated with lignin valorization.

Fixed carbon is defined as the biomass remaining after the release of volatile matter, excluding ash and moisture content. This differs from the ultimate carbon content of the biomass sample, as the carbon loss occurs in the form of hydrocarbons during the release of volatile matter. The ultimate carbon content is liberated in the form of both CO and fixed carbon.

Both the volatile matter and the fixed carbon contents significantly influence the thermochemical conversion process of these wastes. The interplay between these components is highlighted by the ratio of volatile matter to fixed carbon (VM/FC), revealing a noteworthy correlation with the hydrogen content observed in the ultimate analysis.

To further characterize the biomass wastes, the high heating value (HHV), representing the gross calorific value, was determined for all samples. The HHV was calculated based on the ultimate analysis of the three-biomass wastes with the available empirical formula and was found to range from 15.67–17.65 MJ kg^{-1} in the studied biomass wastes.

The thermogravimetric (TG) curves shown in Fig. 3 indicates that the weight loss of the biomass feedstocks ranges between 30 °C and 1000 °C for the 3 samples. TGA can be potentially used to predict the pyrolysis behavior of each tested biomass waste. As deduced from the TG curves, the initial region of weight loss, occurring between room temperature and 190 °C, is mainly attributed to the elimination of moisture content and

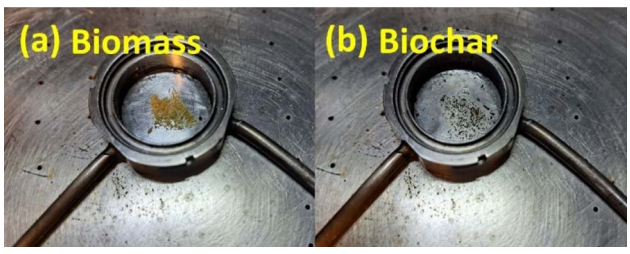

Fig. 2 (a) Overview of the biomass (feathertop plant) in the steel reactor and (b) biochar obtained after photo-pyrolysis at 575 V-pulse and flashing time of 72.5 ms.

Table 1 Proximate analysis, ultimate analyses and composition of biomass wastes

Analysis		Onion waste	*Pennisetum alopecuroides*	*Pennisetum villosum*
Proximate analysis on raw matter	Moisture (*m*%)	44.19	64.31	54.89
	Volatile matter (VM) (*m*%)	39.16	25.91	31.54
	Ash (*m*%)	5.67	4.76	6.59
	Fixed carbon (FC) (*m*%)	10.98	5.02	6.98
	VM/FC	3.84	5.16	4.52
	HHV (MJ kg^{-1})	17.39	17.65	15.67
Ultimate analysis on dry matter	N (%)	1.77	1.85	2.32
	C (%)	45.11	42.43	38.85
	H (%)	4.96	6.23	5.13
	S (%)	0.98	1.64	0.34
	O[a] (%)	41.51	43.09	46.77
Composition	Cellulose (%)	32.23	42.53	29.37
	Hemicellulose (%)	37.33	34.86	51.62
	Lignin (%)	26.75	15.85	12.42

[a] The oxygen content was calculated on the ash free basis.

light volatile matter, particularly water-soluble hydroxyl and carboxyl groups present in the initial biomass waste.[30] The major degradation occurs during the second stage, at temperatures between 190 °C and 440 °C, which can be further divided into two sub-stages. The first sub-stage involves the breakage of glycosidic bonds and thermal depolymerization of non-cellulose groups, such as hemicellulose and pectin, while the second sub-stage is attributed to the decomposition of cellulose constituents.[30,31] During the last stage, with temperatures ranging from 440 °C to 900 °C, the decomposition of residual products shows a slow degradation profile due to the gradual and constant decomposition of the complex lignin compound. The decomposition of lignin occurs at 540 °C. Beyond 900 °C, the remaining residue is considered as biochar, composed of carbon and mineral content. The amount of residual biochar depends on the characteristics of the feedstocks, namely fixed carbon and ash content. The residual biochar for onion waste, *Pennisetum alopecuroides*, and *Pennisetum villosum* was 27%, 17% and 20% of the initial mass, respectively. These observed values are in agreement with the proximate analysis of the three wastes in terms of fixed carbon and ash content (Table 1).

Fig. 3 illustrates the Derivative Thermogravimetric (DTG) curves obtained for the biomass materials. As shown in Fig. 3, all materials exhibited three main peaks, corresponding to the decomposition of hemicellulose, cellulose, and lignin at distinct temperature ranges. Up to a temperature of 250 °C, the mass loss recorded was approximately 23%, 15%, and 13% for the three biomass wastes, respectively, which can be mainly attributed to the removal of moisture during the pyrolysis process. However, since the mass loss value is significantly greater than the moisture content on a dry basis, the removal of some low molecular weight volatile components should also be considered in the mass loss of this first stage, in addition to the moisture removal. Moreover, regarding the mass loss at this first stage, it can be concluded that onion waste releases volatile matter much earlier than the other two biomass wastes.

The second stage was observed between 230 °C and 300 °C, where the respective mass loss rates of 17%, 25%, and 26% for the three biomass wastes were considerably higher compared to the first stage. This is attributed to the initiation of the main devolatilization reactions, characterized by low thermal stability, originating from the degradation of organic compounds in the three biomass wastes. Based on previous studies,[32,33] hemicellulose is decomposed between 220 °C and 330 °C, indicating that this second stage loss can be mainly attributed to hemicellulose degradation.

The third stage of the three biomass wastes occurred between 300 and 425 °C, associated with a mass loss of 26%, 33%, and 27% for onion waste, *Pennisetum alopecuroides*, and *Pennisetum villosum*, respectively. This mass loss was higher than in the previous stages, indicating the continuation of devolatilization reactions. Therefore, the mass loss of the third stage can be attributed predominantly to the thermal degradation of a component with higher thermal stability than

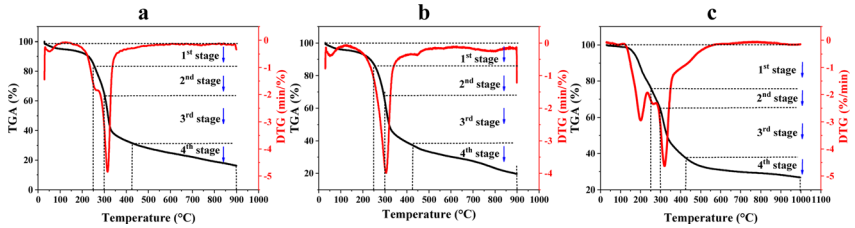

Fig. 3 TGA and DTG curves of (a) *Pennisetum villosum* (b) *Pennisetum alopecuroides* and (c) Onion waste.

hemicellulose. It is reported that cellulose is characterized by high thermal stability with a degradation that occurs mainly in the range of 300 °C to 410 °C.[33,34] Therefore, this third stage can be mainly attributed to cellulose degradation and partial lignin degradation.

The fourth stage occurs between the temperatures of 425 °C and 900 °C and is characterized by a mass loss of 9.4%, 17%, and 15% for the three biomass samples, respectively. The mass loss of this fourth stage can be attributed mainly to the degradation of the most thermally stable component in the structure of the three biomass wastes, which is lignin. Lignin is reported to undergo thermal degradation within a wide temperature range spread between 150 °C and 1000 °C.[33,34]

TGA-DTG analysis is a crucial and potentially informative characterization technique to evaluate the behavior of different biomass wastes during the pyrolysis process. Therefore, from this analysis, it can be concluded that at approximately 500 °C, the majority of volatile compounds are generated, with amounts of 66%, 63%, and 65%, excluding moisture, for the three biomass wastes, respectively. Hence, for liquid (oil) production, a pyrolysis temperature of 500 °C should be sufficient.

The obtained FTIR spectra for the three-biomass waste samples, are presented in Fig. 4, where characteristic absorption bands of the various chemical compounds are shown. A prominent peak at 3343 cm^{-1} was observed in all three spectra, indicating the stretching vibration of O–H bonds in cellulose.[35]

Another strong peak at 1044 cm^{-1} is attributed to C–O stretching vibrations in both hemicelluloses and cellulose. Furthermore, the spectra displayed bands in the region of 1650–1440 cm^{-1}, which are characteristic of C=C bonds. These bands were predominantly associated with aromatic compounds found in lignin, a major component of lignocellulosic materials.[30,36] Additionally, a consistent peak at 1645 cm^{-1} was present in all samples, suggesting the presence of both water molecules and C=O bonds of hemicelluloses. Moreover, a noteworthy peak at 1438 cm^{-1} was observed, indicating the presence of C–H bending vibrations, primarily attributed to cellulose, another integral component of lignocellulosic materials.[37,38] Overall, the observed FTIR bands and functional groups align with the characteristics of lignocellulosic materials, further confirming the nature of the three biomass waste samples. These results are in accordance with reported values on Table 1.

Fig. 5 shows the XRD patterns of the analyzed biomass materials. Cellulose, a structurally pivotal component, is inherently characterized by a coexistence of amorphous and crystalline domains.[39] In contrast, lignin and hemicellulose are predominantly amorphous in nature.[37,38] The overarching lignocellulosic matrix, however, exhibits a multifaceted arrangement wherein the amorphous fraction may be predominant. The significant presence of amorphous regions contributes to a pronounced background signal that obscures the sharp signals arising from crystalline regions.[36,37] The presented XRD findings distinctly illustrate this phenomenon, with a broad peak dominating around 2θ at 20.84° for all samples. The distinctiveness of this broad peak, suggests a semi-crystalline nature of the biomass samples structure.[39] This can be attributed to intricate interactions between the hydroxyl (–OH) groups of cellulose and the carbonyl (C=O) groups of hemicellulose and lignin.[36] Furthermore, differentiation among the XRD profiles of the biomass samples is rooted in their polycrystalline nature, a consequence of varying cellulose content within each sample.[38]

Photopyrolysis

Each biomass waste was subjected to photo-pyrolysis with the conditions described above for a dry matter quantity of 10 mg per test.

As a result of photo-pyrolysis, the 10 mg of onion waste (flower and petiole) resulted in 2 mg of biochar, while the feathertop plant (*Pennisetum alopecuroides*) and the feathertop plant (*Pennisetum Villusom*) yielded 1.9 mg and 2.1 mg, respectively.

Higher temperatures are known to enhance the decomposition of solid waste, promoting secondary reactions that increase the yield of syngas, primarily composed of CH_4, H_2, CO, and CO_2. Consequently, the mass yield of biochar is directly influenced by the intensity and duration of the light flashes. A

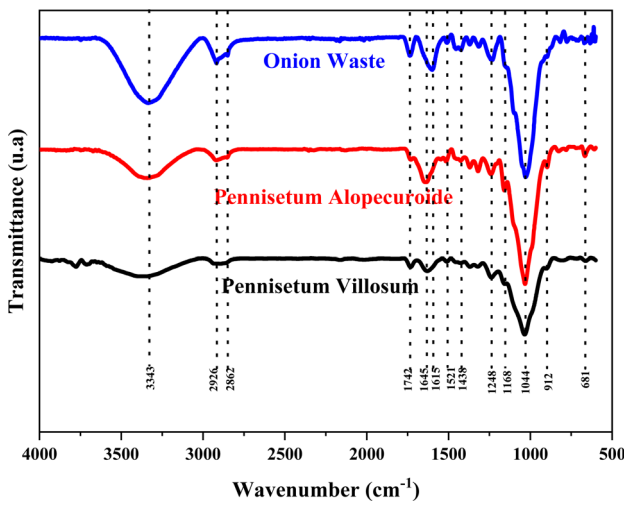

Fig. 4 FTIR spectrum of the biomass wastes.

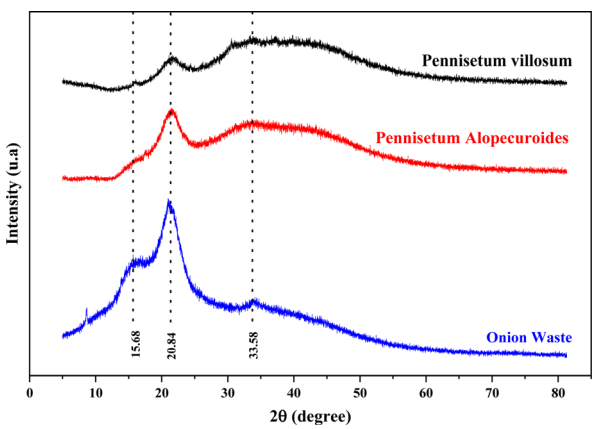

Fig. 5 X-ray diffractogram of the different biomass wastes.

direct correlation between the fixed carbon content of the biomass and the biochar yield[40] was established, as well as the volatile matter content and the bio-oil yield in the photo-pyrolysis process. The differences in the mass of biochar generated between the three photopyrolyzed biomass samples are relatively minor, with approximately 20% of the initial mass remaining after the photo-pyrolysis process.

When considering the TGA-DTG results, the remaining mass fraction of onion waste is the highest, followed by *Pennisetum villusom* and then *Pennisetum alopecuroides*. This trend is consistent with the proximate analysis of the three samples in terms of fixed carbon and ash content, with onion waste having the highest content, followed by *Pennisetum villusom* and *Pennisetum alopecuroides*. These results suggest that the decomposition of the three types of biomass during the photo-pyrolysis process varies, dependent on the processing conditions, mainly temperature. Several studies have shown that pyrolysis temperature is an important parameter that strongly influences product distribution. Moreover, the increase of the process temperature will directly lead to an increase in the thermochemical conversion of the biomass waste resulting in the release of higher quantities of compounds, and thus a lower remaining fraction of biochar. This decrease can be attributed to secondary cracking reactions in the bio-oil, which favors a higher formation of lower molecular weight compounds and gas products. Moreover, high temperature may also led to char residue decomposition. Consequently, the higher biochar yield at lower pyrolysis temperatures indicates incomplete or partial biomass decomposition, thus justifying the slight differences observed in the biochar yield for the three-biomass wastes. It is important to note that the biochar generated in this process is in a liquid–solid state, commonly referred to as 'oily'. Therefore, further treatment is necessary to convert this biochar into a suitable form for applications such as hydrogen storage or CO_2 capture.

Cellulose-rich biomass is better suited for liquid production, whereas biomass rich in hemicellulose is more suitable for syngas production.[41] Biomass with high lignin content, on the other hand, serves as an excellent feedstock for biochar production.[42] However, it is worth noting that many simulations and studies have demonstrated that relying on a single biomass pyrolysis product may not yield favorable economic benefits.[4] Therefore, enhancing the value of by-products, such as biochar

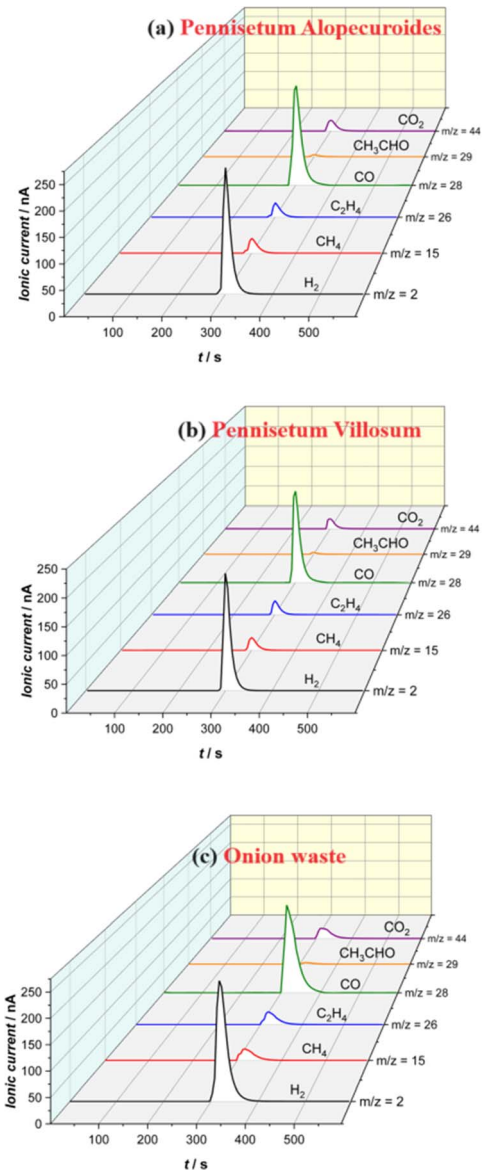

Fig. 6 Ionic currents for m/z 2 (H_2), 15 (CH_4), 26 (C_2H_4), 28 (CO), 29 (CH_3CHO) and 44 (CO_2) obtained during the flash light irradiation at 575 V-pulse and 72.5 ms from different biomass: (a) *Pennisetum alopecuroides*, (b) *Pennisetum villosum* and (c) onion waste.

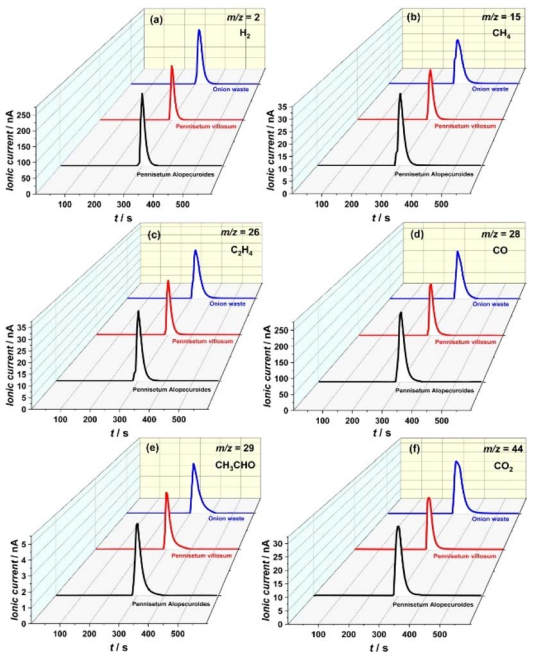

Fig. 7 Comparison of the ionic currents of (a) m/z 2 (H_2), (b) 15 (CH_4), (c) 26 (C_2H_4), (d) 28 (CO), (e) 29 (CH_3CHO) and (f) 44 (CO_2) obtained during the photo-pyrolysis of *Pennisetum alopecuroides*, *Pennisetum villosum* and onion waste by flash light irradiation at 575 V-pulse and 72.5 ms.

Table 2 Number of moles and dry mass composition of the three biomass samples based on 100 g wet samples

	Onion waste		*Pennisetum alopecuroides*		*Pennisetum villosum*	
	Dry mass (g)	Number of moles (mole)	Dry mass (g)	Number of moles (mole)	Dry mass (g)	Number of moles (mole)
Fixed carbon	6.12	0.51	1.8	0.15	3.15	0.26
C	45.11	2.09	42.43	1.26	38.85	1.46
H	4.96	2.77	6.23	2.22	5.13	2.31
$O^{ashfree}$	41.51	1.45	43.09	0.96	46.77	1.32
N	1.77	0.07	1.85	0.04	2.32	0.07

and syngas, becomes a pivotal strategy to mitigate the impact of various biomass feedstocks on the final products.

The gas produced during photo-pyrolysis was analyzed using online mass spectroscopy (MS), and the results are presented in Fig. 6 and 7 for the three biomass wastes. Various gas products are generated during the photopyrolysis process, with a high ionic current attributed to hydrogen and carbon monoxide. The ionic current of acetaldehyde is the lowest, while ethylene, methane, and carbon dioxide fall in the middle range in terms of ionic current. The higher signal intensities for H_2 and CO, and the lower intensities for CO_2, CH_4, C_2H_4, and CH_3CHO collected under the photopyrolysis conditions for the three biomass wastes, suggest that the released gas is a hydrogen-rich gas. The use of biomass wastes in their wet conditions may thermodynamically lead to more hydrogen formation, following the water gas shift reaction ($CO + H_2O \rightleftharpoons CO_2 + H_2$).[2] Several reactions take place during the biomass flash photopyrolysis a series of these reactions are given in the ESI.†

To further understand biomass decomposition during the photopyrolysis process, Table 2 provides a detailed breakdown of the composition of the three biomass wastes in terms of dry mass (dm) and molar number (moles) based on 100 g of each wet sample. Analyzing the compatibility of atoms and mass helps deepen our understanding of the conversion process to produce syngas or hydrogen-rich gas.

If we assume that the oxygen in the 100 g of samples, which amounts to 1.45, 0.96, and 1.32 moles of oxygen atoms present in onion waste, *Pennisetum alopecuroides*, and *Pennisetum villusom*, respectively, is totally used to form CO (see Fig. 6 and 7), the remaining carbon would be 0.64, 0.30, and 0.14 moles for the three wastes, respectively, which is higher than the fixed carbon of the three biomass samples, suggesting that other carbon containing volatile products have been formed.

In addition, the expected maximum number of moles of hydrogen that are used to form H_2 would be 2.77, 2.22, and 2.31 moles for the three biomass samples, respectively. Assuming that the VM is mainly composed of H_2 and CO, the resulting quantities of CO would be 1.22, 0.85, and 0.94 moles for the three samples, respectively. Comparing the generated CO amounts to the molar amount of O in each sample reveals a difference of 0.23, 0.11, and 0.38 moles for the three biomass samples, respectively. Therefore, based on this simple comparison, we conclude that other oxygenated molecules are produced such as CO_2 and CH_3CHO, in addition to perhaps NO_x molecules, which is in qualitative agreement with observed results from the MS analysis.

Conclusion

This study is a contribution to the exploration of biomass feedstock in Morocco to produce high-value products, specifically biochar and syngas or hydrogen-rich gas. The innovative approach was to employ photo-pyrolysis as a screening tool for biomass processing, which enhance the efficiency of this investigation. This rapid pyrolysis process, coupled with Mass Spectrometry (MS), not only rivals the classical ultimate analysis but also yields more comprehensive results compared to established pyrolysis techniques such as TGA-MS and FTIR-MS.

The analysis of the gas composition from three distinct biomass wastes in this study provides crucial insights into their thermochemical characteristics. The application of photo-pyrolysis, with its rapid and informative capabilities, not only enhances our understanding of these characteristics but also creates paths for optimizing the conversion of biomass into valuable energy products, thereby contributing to carbon mitigation efforts.

The results obtained from this study play a dual role, expanding our knowledge of the potential of Moroccan biomass resources for carbon and syngas or hydrogen-rich gas production, while also advancing the characterization process of waste materials. This enhanced characterization is pivotal in revealing the potential of these wastes in the renewable energy sector.

Author contributions

A. Mellalou: conceptualization, formal analysis, investigation, methodology, validation, writing – original draft. Wanderson O. Silva: conceptualization, formal analysis, investigation, methodology, writing – review & editing. Mathieu Soutrenon: formal analysis, investigation, writing – review & editing. Hubert H. Girault: formal analysis, investigation, supervision, writing – review & editing. A. Outzourhit: formal analysis, supervision, writing – review & editing. J. Alami: formal analysis, funding acquisition, writing – review & editing. F. Ghamouss: formal analysis, funding acquisition, investigation, validation, supervision, writing – review & editing.

Conflicts of interest

There are no conflicts to declare.

Acknowledgements

The authors would like to acknowledge Office Chérifien des Phosphates (OCP) for financing this work.

Notes and references

1 F. Guo, Y. Dong, B. Tian, S. Du, S. Liang, N. Zhou, Y. Wang, P. Chen and R. Ruan, *Sustainable Energy Fuels*, 2020, **4**, 5927–5946.
2 D. B. Pal, A. Singh and A. Bhatnagar, *Int. J. Hydrogen Energy*, 2022, **47**, 1461–1480.
3 X. Zhang, K. Rajagopalan, H. Lei, R. Ruan and B. K. Sharma, *Sustainable Energy Fuels*, 2017, **1**, 1664–1699.
4 Y. S. Zhang, H. L. Zhu, D. Yao, P. T. Williams, C. Wu, D. Xu, Q. Hu, G. Manos, L. Yu, M. Zhao, P. R. Shearing and D. J. L. Brett, *Sustainable Energy Fuels*, 2021, **5**, 4173–4208.
5 Y. Shen and Y. Fu, *Sustainable Energy Fuels*, 2018, **2**, 326–344.
6 B. Dou, H. Zhang, Y. Song, L. Zhao, B. Jiang, M. He, C. Ruan, H. Chen and Y. Xu, *Sustainable Energy Fuels*, 2019, **3**, 314–342.
7 V. Dieterich, A. Buttler, A. Hanel, H. Spliethoff and S. Fendt, *Energy Environ. Sci.*, 2020, **13**, 3207–3252.
8 V. G. Nguyen, T. X. Nguyen-Thi, P. Q. Phong Nguyen, V. D. Tran, Ü. Ağbulut, L. H. Nguyen, D. Balasubramanian, W. Tarelko, S. A. Bandh and N. D. Khoa Pham, *Int. J. Hydrogen Energy*, 2024, **54**, 127–160.
9 P. P. Singh, A. Jaswal, R. Singh, T. Mondal and K. K. Pant, *Int. J. Hydrogen Energy*, 2024, **50**, 627–639.
10 S. García-casado, R. Muñoz and R. Lebrero, *Bioresour. Technol.*, 2024, 130646.
11 Y. Shen, D. Ma and X. Ge, *Sustainable Energy Fuels*, 2017, **1**, 1700–1729.
12 M. I. Taipabu, K. Viswanathan, W. Wu, N. Hattu and A. E. Atabani, *Process Saf. Environ. Prot.*, 2022, **164**, 384–407.
13 M. Belmakki, E. H. Bartali and H. Xiaoru, *Identifcation and characterization of organic waste in Morocco an important step towards the valorization of waste*, Rev Mar Sci Agron Vét, 2015, 3, pp. 37–45.
14 Morocco Wants To Transform Its Biomass Into Energy, **https://www.moroccoworldnews.com/2021/10/345012/morocco-wants-to-transform-its-biomass-into-energy**, accessed 4 April 2023.
15 P. R. Lanjekar, N. L. Panwar and C. Agrawal, *Bioresour. Technol. Rep.*, 2023, **21**, 101293.
16 W. O. Silva, B. Nagar, M. Soutrenon and H. H. Girault, *Chem. Sci.*, 2022, **13**, 1774–1779.
17 W. O. Silva, B. Nagar, D. Ellersiek, L. Bondaz, J. Espín, M. Soutrenon and H. H. Girault, *Sustainable Energy Fuels*, 2023, **7**, 5693–5703.
18 B. Nagar, M. Jović, V. C. Bassetto, Y. Zhu, H. Pick, P. Gómez-Romero, A. Merkoçi, H. H. Girault and A. Lesch, *ChemElectroChem*, 2020, **7**, 460–468.
19 D. Reynard, B. Nagar and H. Girault, *ACS Catal.*, 2021, **11**, 5865–5872.
20 H. W. Cui, J. T. Jiu, T. Sugahara, S. Nagao, K. Suganuma, H. Uchida and K. A. Schroder, *J. Therm. Anal. Calorim.*, 2015, **119**, 425–433.
21 A. Ignat, L. Manzocco, M. Maifreni, I. Bartolomeoli and M. C. Nicoli, *Postharvest Biol. Technol.*, 2014, **91**, 122–127.
22 K. Sharma, N. Mahato, S. H. Nile, E. T. Lee and Y. R. Lee, *Food Funct.*, 2016, **7**, 3354–3369.
23 Morocco Onion Industry Outlook 2022–2026, **https://www.reportlinker.com/clp/country/3697/726328**, accessed 30 July 2023.
24 M. A. Salem, H. E. A. Mansour, E. M. Mosalam, R. A. El-Shiekh, S. M. Ezzat and A. Zayed, *Valorization of By-Products Derived from Onions and Potato: Extraction Optimization, Metabolic Profile, Outstanding Bioactivities, and Industrial Applications*, Springer, Netherlands, 2023, vol. 14.
25 A. Ouensanga, *Wood Fiber Sci.*, 1989, **21**, 105–111.
26 iTeh Stand, *Technical Association of Pulp and Paper Industry Standard Method T 222-om-83*, 2022, vol. 4, p. 19428.
27 L. Boopathi, P. S. Sampath and K. Mylsamy, *Composites, Part B*, 2012, **43**, 3044–3052.
28 Z. T. Yu, X. Xu, Y. C. Hu, L. W. Fan and K. F. Cen, *Fuel*, 2011, **90**, 1128–1132.
29 M. El Achaby, Z. Kassab, A. Barakat and A. Aboulkas, *Ind. Crops Prod.*, 2018, **112**, 499–510.
30 A. Ahmed, S. Hidayat, M. S. Abu Bakar, A. K. Azad, R. S. Sukri and N. Phusunti, *Biofuels*, 2021, **12**, 9–20.
31 J. W. Rhim, J. P. Reddy and X. Luo, *Cellulose*, 2015, **22**, 407–420.
32 G. Palareti, C. Legnani, B. Cosmi, E. Antonucci, N. Erba, D. Poli, S. Testa and A. Tosetto, *Comparison between Different D-Dimer Cutoff Values to Assess the Individual Risk of Recurrent Venous Thromboembolism: Analysis of Results Obtained in the DULCIS Study*, 2016, vol. 38.
33 E. Müsellim, M. H. Tahir, M. S. Ahmad and S. Ceylan, *Appl. Therm. Eng.*, 2018, **137**, 54–61.
34 G. Palareti, C. Legnani, B. Cosmi, E. Antonucci, N. Erba, D. Poli, S. Testa and A. Tosetto, *Int. J. Lab. Hematol.*, 2016, **38**, 42–49.
35 X. Ouyang, W. Wang, Q. Yuan, S. Li, Q. Zhang and P. Zhao, *RSC Adv.*, 2015, **5**, 61650–61656.
36 M. Poletto, H. L. Ornaghi Júnior and A. J. Zattera, *Materials*, 2014, **7**, 6105–6119.
37 B. de Diego-Díaz, A. Duran, M. R. Álvarez-García and J. Fernández-Rodríguez, *Fuel*, 2019, **245**, 240–246.
38 E. Ahmed, A. Zeitoun, G. Hamad, M. A. M. Zeitoun, A. Taha, S. A. Korma and T. Esatbeyoglu, *Foods*, 2022, **11**, 1–16.
39 L. K. Herrera, A. Justo, A. Duran, M. C. Jimenez De Haro, M. L. Franquelo and J. L. Perez Rodríguez, *Appl. Phys. A: Mater. Sci. Process.*, 2010, **99**, 391–398.
40 S. G. C. de Almeida, L. A. C. Tarelho, T. Hauschild, M. A. M. Costa and K. J. Dussán, *Chem. Eng. Process.*, 2022, **179**, DOI: **10.1016/j.cep.2022.109054**.
41 A. Iaccarino, R. Gautam and S. M. Sarathy, *Sustainable Energy Fuels*, 2021, **5**, 2234–2248.
42 Z. Pan, A. Puente-Urbina, A. Bodi, J. A. van Bokhoven and P. Hemberger, *Chem. Sci.*, 2021, **12**, 3161–3169.